

Experimental testing of multi-tubular reactor for hydrogen production and comparison with a thermal CFD model

Cite as: AIP Conference Proceedings **2033**, 130013 (2018); <https://doi.org/10.1063/1.5067147>
Published Online: 08 November 2018

Elvira Tapia, Aurelio González-Pardo, Alfredo Iranzo, Alfonso Vidal, and Felipe Rosa



View Online



Export Citation

ARTICLES YOU MAY BE INTERESTED IN

[Thermal tests of a multi-tubular reactor for hydrogen production by using mixed ferrites thermochemical cycle](#)

AIP Conference Proceedings **1850**, 100009 (2017); <https://doi.org/10.1063/1.4984466>

[Heliostat aiming strategy of 3 cylindrical cavity-receivers integrated in a 750 kW solar tower hydrogen plant](#)

AIP Conference Proceedings **2033**, 130007 (2018); <https://doi.org/10.1063/1.5067141>

[HYDROSOL-PLANT: Structured redox reactors for H₂ production from solar thermochemical H₂O splitting](#)

AIP Conference Proceedings **2033**, 130010 (2018); <https://doi.org/10.1063/1.5067144>

AIP | Conference Proceedings

Get **30% off** all
print proceedings!

Enter Promotion Code **PDF30** at checkout



Experimental Testing of Multi-Tubular Reactor for Hydrogen Production and Comparison with a Thermal CFD Model

Elvira Tapia^{1,a)}, Aurelio González-Pardo^{2,b)}, Alfredo Iranzo^{1,c)}, Alfonso Vidal^{2,d)},
Felipe Rosa^{1,e)}

¹*Thermal Engineering Group, Energy Engineering Department. School of Engineering, University of Seville. Camino de los Descubrimientos s/n, 41092 Sevilla, Spain.*

²*CIEMAT-PSA, Carretera de Seners, S/N Tabernas, Almería, Spain.*

^{a)}Corresponding author: etapia@us.es

^{b)}aurelioj@psa.es

^{c)}airanzo@us.es

^{d)}alfonso.vidal@ciemat.es

^{e)}rosaf@us.es

Abstract. This study presents a comparison of the experimental tests and CFD results for a multi-tubular solar reactor for hydrogen production in a pilot plant in the Plataforma Solar de Almería. This paper describes the methodology used for the solar reactor design and the experimental tests carry out during the testing and characterization campaign of the plant. The CFD model which has been used to design the solar reactor has been validated with an error around 10%. CFD simulations also allow to solve the thermal balance in the reactor (cavity and tubes) and to calculate the percentage of reacting media inside the tubes which achieve the required temperature for the process. The temperature in the thermocouples is around 1200 °C for the experimental data and a 90% of the ferrite inside the tube is above 900 °C. The multi-tubular solar reactor, which has been design with CFD techniques, has been built and operated successfully.

INTRODUCTION

Technologies involving high temperature endothermic reactions for converting solar energy to chemical fuels have been investigated around the world. Many of the activities are focused on identifying, developing, and assessing improved receiver/reactors for efficiently carrying out the thermochemical processes for the production of hydrogen [1]. In this context, solar reactors represent a promising technology for a sustainable energy system, for example as an energy storage by producing an energy carrier (hydrogen) for its use during the period when solar energy is not available. At present, different solar reactors have been demonstrated for different chemical processes and scales.

Nowadays, CFD tools are increasingly being used for solar reactors design and to optimize operating conditions. The studies using CFD tools have increased during the last years in order to better predict results of temperature, heat flux, pressure, and velocity distributions. Different reactor types and configurations are possible, and clearly the modelling requirements and details will vary depending on the reactor type.

A 100 kWth multi-tubular cavity reactor for hydrogen production integrated in a solar tower was designed, manufactured and tested in the framework of a project called SolH2 (an INNPACTO initiative of the Spanish Ministry of Economy and Competitiveness) with the main goal to demonstrate the technological feasibility of solar thermochemical water splitting cycles as one of the most promising options to produce hydrogen from renewable

sources in an emission-free way. At the end of this project, the ownership of this plant has been transferred to CIEMAT for further in-depth studies.

The reactor was designed according to the receiver requirements of the capacity for a given hydrogen production, inlet and outlet gas temperatures, and efficiency. A Computational Fluid Dynamic (CFD) analysis of the solar cavity-receiver was carried out within the design process to determine and optimize the temperature distribution and the absorbed radiation flux over the internal cavity walls, which is explained in the next section. In this work, the CFD modelling for the 100 kW (commercial scale) multi-tubular reactor design is validated with the experimental results of this pilot plant in the Plataforma Solar de Almería (PSA).

PILOT PLANT

The reactor has been installed in the SSPS-CRS facility of the Plataforma Solar de Almería, located in Tabernas desert, Spain. The Plataforma Solar de Almería is the largest European solar energy research center with more testing facilities in the world of solar energy. The SSPS-CRS plant consists of an autonomous field of heliostats and a metallic tower 43 meters high. The facility collects direct solar radiation by means of a field of 91 39.3-m² -surface heliostats distributed in a 150-x- 70-m north field into 16 rows. The tower is 43 meters high and has two metal testing platforms, at 26 and 32 meters respectively. The maximum thermal power delivered by the field onto the receiver aperture is 2,0 MW. This plant has been used in the past to accommodate testing of small solar receivers in the range of 200-350 kW thermal power applications. Nowadays, the test facility has been turned into a suitable test-bed to host the most important research initiatives in solar hydrogen production: HYDROSOL –Plant, SYNPET, etc.

Reactor

According to the hydrogen production specifications and the initial geometry conditions, a first design for the solar reactor was proposed. This initial design consisted of a semi-cylindrical cavity with 2 m radius and a square opening 30x30 cm². Inside the cavity there were 80 tubes in a staggered arrangement in 2 rows (FIGURE 1 (a)). This design was dismissed for two main reasons: the empty space in the middle of the rows in front of the opening, and the too small opening according to the incident radiation, resulting in an increase of the temperature difference within tubes.

The next reactor was designed to avoid the problems which were found in the initial design. In this case, the opening was increased until 46x46 cm² and the tubes distribution was modified. In this case, it was proposed 3 rows in staggered arrangement increasing the number of tubes until 104 and using the extreme tubes as a preheating interchanger (see FIGURE 1 (b)). This design was dismissed too because the big cavity radius involved a slow transient thermal heating, and the efficiency in extreme preheating interchanger was low.

The final design consists of a semi-cylindrical shape with a 1.5 m internal radius and 80 tubes in staggered arrangement in three rows, including tubes in front of the opening (see FIGURE 1 (c)).

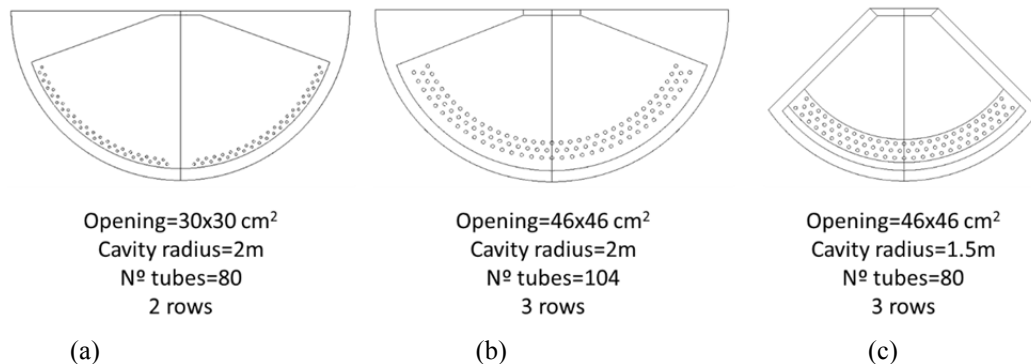


FIGURE 1. (a) Initial solar reactor design. (b) Middle solar reactor design. (c) Final solar reactor design.

All designs were calculated with CFD tools using a Monte Carlo surface-to-surface radiation model to compare the results of incident radiation flux on the walls and on the tubes, and the resulting temperature distributions. The last design was built as result of SolH2 project (see FIGURE 2). The tubes have a length of 1.2 m and a total volume capacity of 566 cm³. These tubes are filled with small pellets of mixed ferrites, cylindrically shaped in order to increase the reaction surface and benefit the gas flow through them.

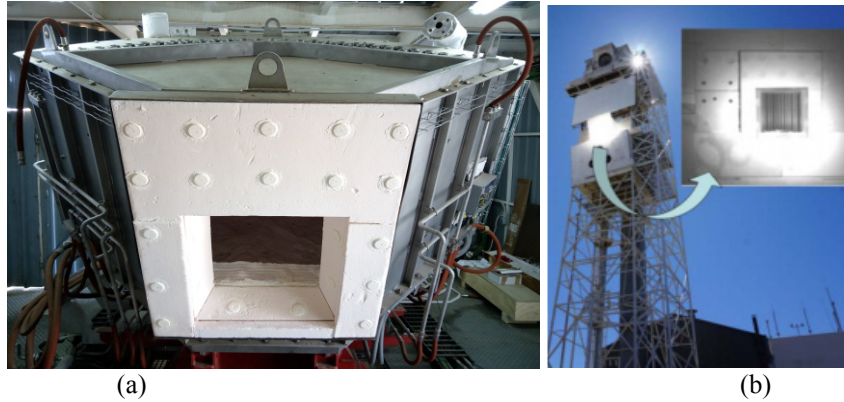


FIGURE 2. (a) Frontal view of the reactor installed in CRS tower plant. (b)View of the reactor being irradiated by CRS field.

Flux Measurement System

This system is used to measure the power arriving to the aperture of the reactor. It consists of capturing the irradiance distribution on a moving lambertian target with a high resolution CCD camera [2]. The bar intercepts the concentrated beam in the measuring plane, which is as close to the receiver as possible. The distribution of relative intensity, in terms of gray-scale map, represents the shape of the flux distribution at the receiver. A radiometer is used to calibrate the system, by correlating the gray-scale values of the image pixels with the corresponding irradiance value measured by the radiometer.

Furthermore, four thermocouples are included inside the tubes to compare the experimental tests with the CFD results. These thermocouples are installed in the middle of the tube, their positions are tube 14 and 21 in the first row and tube 3 and 12 in the second one.

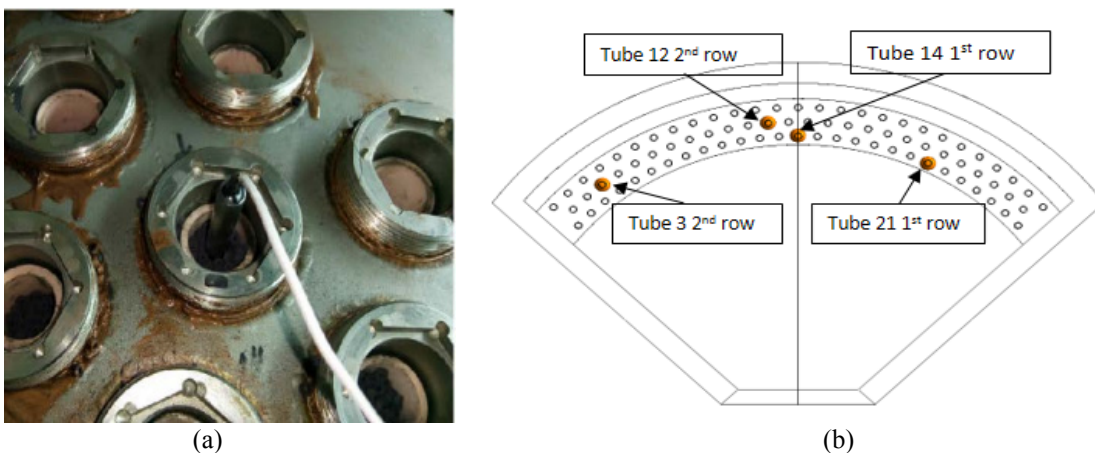


FIGURE 3. (a) Detailed view of the tubes filled with ferrites and with a thermocouple installed. (b) Distribution of the four thermocouples arranged inside the tubes.

THERMAL TESTS

Previous experience with alumina tubes showed that they were very sensitive to temperature gradients. In previous tests, some tubes were broken due to the temperature gradient throughout their length, which produced a stress in the alumina tubes. This evidence and the goal of the design to obtain as homogeneous as possible flux distribution did necessary a good strategy for the heliostats field. Initially, two groups of heliostats were focused on the aperture and then the number of groups was increased until the required temperature was achieved. For the first groups of heliostats, the heating was very progressive, and we did not wait until the temperatures stabilized since it would have taken a long time. When 20 heliostats were focused, a total power of 44.1 kW was focused inside the cavity and a temperature of 750-800 °C was reached. Finally, with a total of 36 heliostats and a power about 80 kW, 1200 °C were reached [3]. In addition, this solar reactor design concept implied a discontinuous hydrogen production over the operation time. Therefore, a sequential mode inside the solar reactor was implemented to couple the operation of the plant with the mixed ferrites thermochemical cycle, which consists of two reaction stages.

This study was done the vernal equinox, which is a representative day of the year. The test was carried out with nitrogen and without water, the total mass flow inside tubes was 40 kg/h and the inlet temperature around 70 °C. The process to focus the groups of heliostats is described below, and it was designed to enable the solar radiation to impinge on all the ceramic tubes: first one, the groups 1 and 2; Then the group 3 and is continued with groups 4 and 5. This part is done very progressive without waiting the stability of temperature. Then, groups 10 and 11 are included and finally groups 8 and 9 (see FIGURE 4). Each group contains distant and nearby heliostats to favor the flux homogeneity [3]. The final configuration of heliostats allows to measure the incident radiation flux and direction of rays at the opening which have been used in CFD simulations.

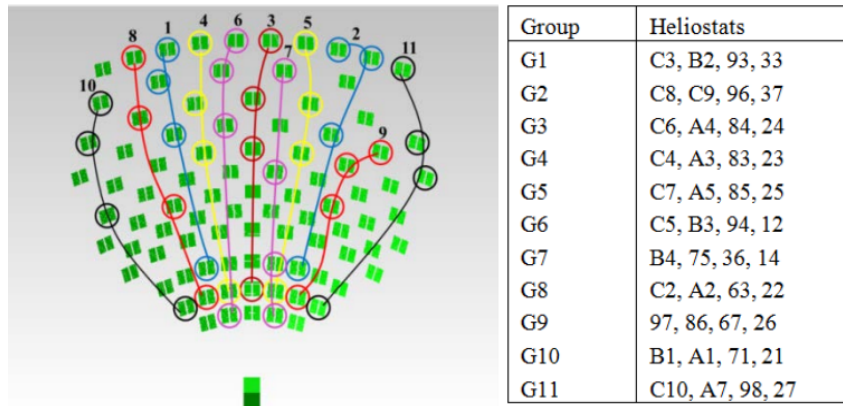


FIGURE 4. Groups of heliostats in which the field has been divided.

CFD MODEL

The commercial software ANSYS-CFX 14.0 [4] has been used to solve the thermal interchanges that exist in the solar multi-tubular reactor. The geometry of the reactor and the operating conditions (radiation flux at opening and mass flow and temperature for the inert gas) are required for solving this methodology [1]. The methodology is focused on a tubular solar reactor where fluid-dynamic model (cavity turbulence) and thermal models (conduction, convection and radiation) are considered in the reactor modeling. In this context, this methodology proposes the Shear Stress Transport (SST) model for turbulence resolution due to the cavity is opened and a better accuracy is achieved in the thermal boundary layer. For radiation model, Monte Carlo model and S2S (surface-to-surface) model are proposed due to the matrix of rays (real directions of a radiation distribution at the opening) is included at the opening, and nonparticipating media is considered. For a proper CFD analysis, it is necessary to previously carry out a mesh analysis in order to ensure that results are independent of the mesh used in the simulations. The main steps are described below:

- The cavity design is focused on optical efficiency and the achievement of a uniform temperature distribution, with a minimum temperature greater than the required temperature for the hydrogen production process. This part of the methodology is divided into different parts where mesh independence analysis, radiation factor independence analysis and boundary conditions are included in the model. A radiation factor independence analysis is required in order to ensure that the number of histories used in the Monte Carlo model is enough to correctly calculate the radiation and temperature field (i.e. a higher number of histories do not influence the results).
- The reactor design starts once the cavity design is closed. The main goals are a complete balance of phenomena which take part in the process, identifying hot/cold spots, and determining the reaction volume which achieves the required conditions.

In order to obtain the optimized computational mesh, grid independence tests are conducted on the mesh models at the beginning of the simulation process. The mesh is refined near wall and high (temperature and velocity modulus) gradient regions. After mesh and radiation factor analysis are done, it is concluded that the final mesh has 1.9 million nodes and 9.0 million elements and the minimum radiation factor (number of histories in the Monte Carlo model) is $125 \cdot 10^6$, which is clearly higher than the default value of $1 \cdot 10^4$.

The concentrated solar radiation enters the cavity receiver through the opening. The incident radiation flux and direction vectors are provided by CIEMAT according to the experimental tests (see FIGURE 5). The total solar power is around 80 kW.

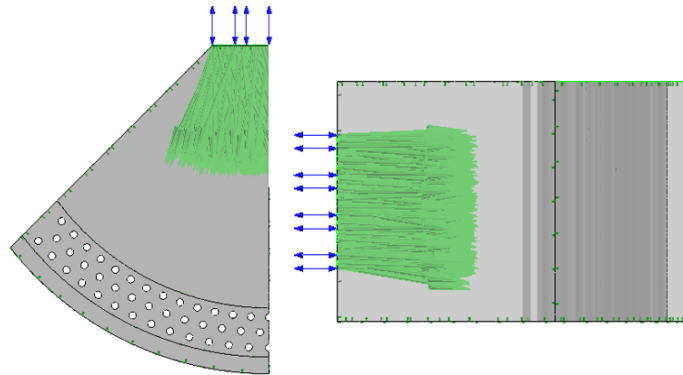


FIGURE 5. Direction of radiation reflected from CRS field (36 heliostats).

A carrier gas, nitrogen, enters the inlet collector located on the top of the reactor and goes through the tubes until the outlet collector. The fluid flow inside the cavity and tubes, air and nitrogen respectively, is assumed as turbulent and laminar respectively, ideal gas and transparent to radiation. Reactor walls are considered as diffusely emitting and reflecting, and opaque. The Monte Carlo model with surface to surface radiation model is used. The conduction heat transfer within the tubes and porous media (ferrite pellets) is included in the same simulation where the radiation behavior is analyzed, therefore avoiding the need for decoupling the models. The specific heat capacity of the nitrogen gas at constant pressure is 1041 J/kgK and dynamic viscosity, density and thermal conductivity are included depending on the temperature as an ideal gas. The thermal conductivity of alumina and silicon carbide are included depending on temperature. The surface emissivity of the diffusely-reflecting cavity inner wall (silicon carbide) and the tubes (alumina) are 0.3 and 0.8 respectively. The nitrogen gas conditions (flow rate and temperature) are the same as the experimental test. The effect of the cavity insulation at the external walls is included in the model, by defining an external heat transfer coefficient of $0.128 \text{ W/m}^2\text{K}$ (equivalent to the insulation material heat conduction resistance and external heat convection resistance).

The summary of physical models and boundary conditions used in the simulation is presented in TABLE 1.

TABLE 1. Physical models and boundary conditions used in the CFD model.

	Model / Boundary Condition value
Radiation model (cavity air)	Monte Carlo / Surface-to-Surface
Turbulence model (cavity air)	Shear Stress Transport (SST)
Turbulence model (nitrogen porous media tubes)	Laminar
Ferrite porosity in tubes	0.4
Cavity window (air)	Opening Boundary Condition [4]
Cavity window (radiation)	Ray matrix profile (direction and intensity) defined from experimental data. 80kW
Tubes emissivity	0.8 (alumina)
Receiver walls emissivity	0.3 (silicon carbide)
Receiver external walls	0.128 W/m ² K, 25°C
Nitrogen tubes inlet	40 kg/h; 70°C

RESULTS

The comparison between the experimental tests and the CFD model results is shown in this section, also aimed at providing an experimental validation of the CFD model. The evolution of temperatures during the experimental test until achieving the steady state for the final configuration of the heliostat field (80 kW) and the steady state CFD results are presented in FIGURE 6. The maximum temperature difference is obtained at tube 21 for the first row and tube 3 in the second row. These tubes are located close to the cavity extremes so the incident radiation flux is lower than at the middle cavity tubes. A further analysis for the direction radiation flux and the opening mesh needs to be done.

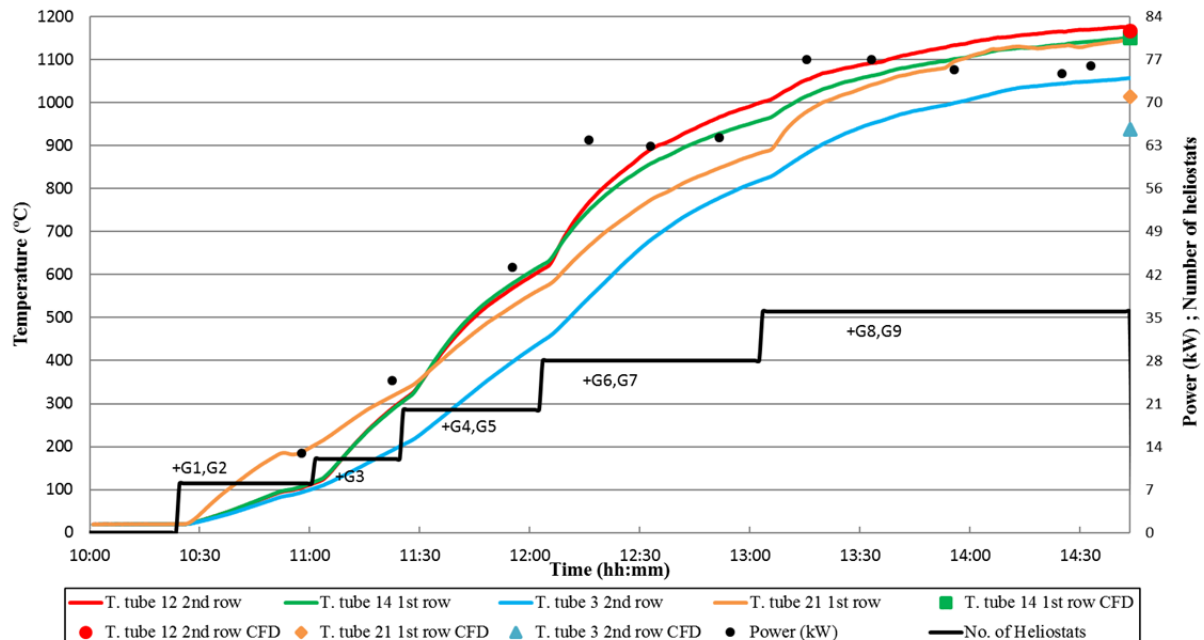


FIGURE 6. Evolution of temperatures for experimental test and CFD temperature results. T. tube corresponds to the thermocouple inside the tubes, in contact with ferrites. Number of heliostats focused on the receiver and the power measured.

The error for the CFD simulation is shown in TABLE 2. It is observed that the CFD temperature results are smaller than the experimental temperature data for all thermocouples, this fact could be caused by larger convection losses in the CFD simulations than in the real experimental tests, as well as difference between the considered and real material emissivity. The maximum temperature error in CFD simulations is around 11.5% which is in the same range as others studies [5, 6, 7, 8]. It can be also observed that errors are very small at central tubes, and larger at the side tubes. The reason for this difference is under investigation. As the incident radiation received by central and side tubes is not the same (mainly direct incident radiation from the heliostat field for central tubes, and reflections and receiver emissions for side tubes) it is possible that either the material emissivity or the accuracy of the radiation model is not fully appropriate for representing the real radiation field within the cavity. This is however still under investigation in order to better assess the reason for this behavior.

TABLE 2. Comparison of experimental temperature and CFD results

	Experimental test (°C)	CFD results (°C)	Error (%)	Difference (K)
T. tube 12 1 st row	1178	1167	0.1	1
T. tube 14 2 nd row	1151	1150	0.9	11
T. tube 21 1 st row	1147	1015	11.5	132
T. tube 3 2 nd row	1058	938	11.3	120

The CFD simulations also allow to evaluate the temperature distribution in tubes. FIGURE 7 (a) shows that temperature in tubes located in cavity extremes are lower than the rest of the tubes. In addition, the effect of the carrier gas mass flow inlet temperature is observed, as the upper part of tubes is clearly colder. FIGURE 7 (b) presents the average temperature at the outer surface of the tubes. All tubes are above 900 °C. It is observed that the second row has the same behavior as the third row near the cavity extremes and the first row in the middle cavity tubes due to the effect of reflexing radiation flux and direct radiation flux respectively. Finally, the temperature difference among different tubes is around 140 °C. So the temperature distribution can be considered homogenous inside the cavity.

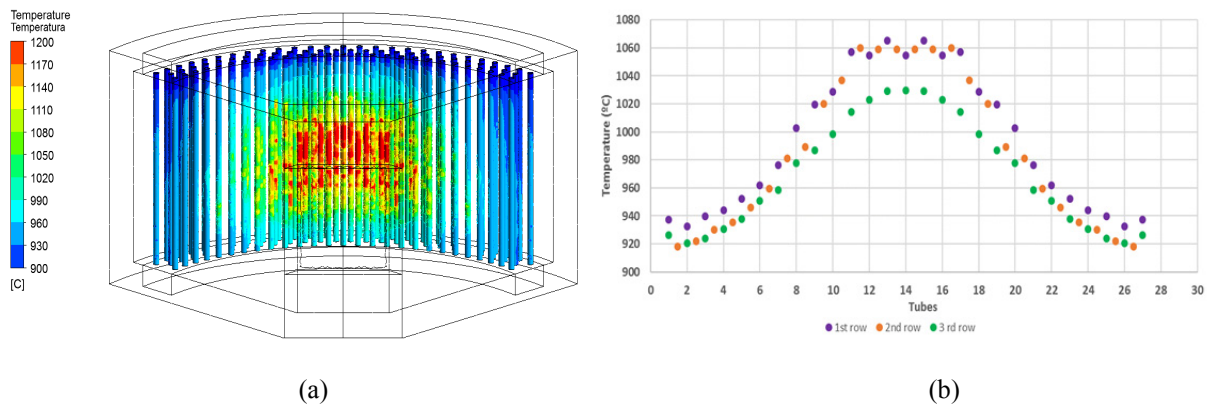


FIGURE 7. (a) Temperature distribution of CFD simulations. (b) Average temperature in the tube surfaces distribution.

The volume of ferrite which achieves the required process temperature is calculated also from the CFD results, and depicted in FIGURE 8. This result is used to analyze the efficiency of the reactor reaction volume. In this case, 90.4% of the ferrite domain achieves the required process temperature (900 °C). This percentage could be further improved if the energy of the outlet carrier gas flow is used to preheat the inlet nitrogen flow.

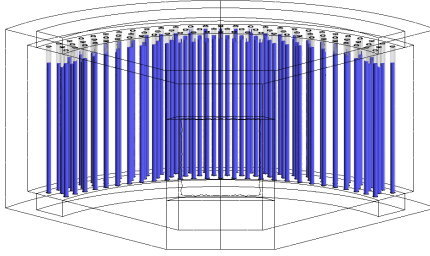


FIGURE 8. Volume of ferrite (inside tubes) where temperature is higher than 900 °C.

The thermal balance is shown in TABLE 3. There are radiation and convection losses in the opening of the cavity, representing around 19 kW and 13 kW respectively. Furthermore, only 6.3 kW are reaching the reaction media inside the tubes. Therefore, the thermal efficiency of the solar reactor is 7.9%.

TABLE 3. Thermal balance in solar reactor

		CFD results
Incident radiation (W)		80000
Opening radiation losses (W)		19032
Opening convection losses (W)		12816
Heat transfer to tube		6340
Optical efficiency (%)	$\eta_{op} = \frac{IncRad - Rad\ losses}{IncRad}$	76.21
Thermal efficiency (%)	$\eta_t = \frac{Heat\ transfer\ to\ process}{IncRad}$	7.93

CONCLUSIONS

A multi-tubular solar reactor designed with the aid of CFD tools was experimentally evaluated during this work. The CFD results on the thermal analysis of the multi-tubular solar reactor are presented in this work, as well as the results of the experimental testing. The purpose of this analysis is to investigate the thermal receiver performance and its operational behavior in the specified conditions. For this specific work, the operation temperatures range from 800 to 1200 °C according to the ferrite cycle. An operation strategy previously performed by ray tracing simulations was applied to supply the required power with the optimal flux distribution onto the alumina tubes. The CFD model was used for the calculation of the temperature and radiation flux profiles at the cavity and receiver walls, and was validated based on the results of the thermal testing campaign. In addition, the temperature distribution inside the tubes was calculated in order to analyze its homogeneity and whether the required temperature is achieved. The scope of the analysis is to assess the thermal efficiency as well as temperatures over the receiver. The validated CFD model provides useful information for the assessment of design parameters and to optimize the thermal performance of the solar cavity.

ACKNOWLEDGMENTS

The authors would like to thank the Spanish Ministry of Science and Innovation (National Plan for Scientific Research, Development and Technological Innovation, 2008-2011), the European Regional Development Fund (ERDF) for the financial support given to the SolH2 project (IPT- 2011-1323-920000) and the FEDER Operational Program for Andalusia 2007-2013 for the financial support given to the RNM 6127 project.

REFERENCES

1. E. Tapia, A. Iranzo, F.J. Pino, et. al. Methodology for thermal design of solar tubular reactors using CFD techniques, [International Journal of Hydrogen Energy](#), Volume 41, Issue 43, (2016), 19525-19538.
2. J. Ballestrín, R. Monterreal. Hybrid heat flux measurement system for solar central receiver evaluation. [Energy](#) 29, 915-924 (2004).
3. A. González-Pardo, T. Denk, A. Vidal. Thermal Tests of a Multi-Tubular Reactor for Hydrogen Production by Using Mixed Ferrites Thermochemical Cycle. SolarPACES Conference Proceedings, 2016, Abu Dhabi, UAE.
4. Ansys Inc., "ANSYS CFX-Solver Theory Guide," ANSYS., USA, 2011, p. 402.
5. D. Hirsch and A. Steinfeld, "Solar hydrogen production by thermal decomposition of natural gas using a vortex-flow reactor," [Int. J. Hydrogen Energy](#), vol. 29, no. 1, pp. 47–55, 2004.
6. H. H. Klein, J. Karni, R. Ben-Zvi, and R. Bertocchi, "Heat transfer in a directly irradiated solar receiver/reactor for solid–gas reactions," [Sol. Energy](#), vol. 81, no. 10, pp. 1227–1239, 2007.
7. N. Ozalp and D. JayaKrishna, "CFD analysis on the influence of helical carving in a vortex flow solar reactor," [Int. J. Hydrogen Energy](#), vol. 35, no. 12, pp. 6248–6260, 2010.
8. S. Bellan, E. Alonso, F. Gomez-Garcia, C. Perez-Rabago, J. Gonzalez-Aguilar, and M. Romero, "Thermal performance of lab-scale solar reactor designed for kinetics analysis at high radiation fluxes," [Chem. Eng. Sci.](#), vol. 101, no. 0, pp. 81–89, 2013.